

Proposal to the ISOLDE and neutron Time-of-Flight Experiment Committee

## Nuclear structure studies of the neutron-rich Rubidium isotopes using Coulomb excitation.

G. Georgiev<sup>1</sup>, J.M. Daugas<sup>2</sup>, G. Simpson<sup>3</sup>, D.L. Balabanski<sup>4</sup>, A. Blazhev<sup>5</sup>, D. Bucurescu<sup>6</sup>,  
S. Das Gupta<sup>7</sup>, T. Faul<sup>2</sup>, D. Filipescu<sup>6</sup>, E. Fiori<sup>1</sup>, L. Gaudefroy<sup>2</sup>, D. Ghita<sup>6</sup>, M. Hass<sup>8</sup>,  
K. Hauschild<sup>1</sup>, D. Jenkins<sup>9</sup>, U. Koester<sup>10</sup>, T. Kroel<sup>11</sup>, V. Kumar<sup>8</sup>, G. Lo Bianco<sup>7</sup>,  
N. Marginean<sup>6</sup>, A. Lopez-Martens<sup>1</sup>, C. Mihai<sup>6</sup>, R. Lozeva<sup>1</sup>, V. Meot<sup>2</sup>, D. Mücher<sup>5</sup>, P. Reiter<sup>5</sup>,  
O. Roberts<sup>9</sup>, O. Roig<sup>2</sup>, M. Seidlitz<sup>5</sup>, K. Singh<sup>8</sup>, A. Stuchbery<sup>12</sup>, D. Voulot<sup>13</sup>, J. Van de Walle<sup>13</sup>,  
N. Warr<sup>5</sup>, F. Wenander<sup>13</sup>, A. Wendt<sup>5</sup>  
and REX-ISOLDE and Miniball collaborations

1. CSNSM, Orsay, France
2. CEA/DIF/DPTA/SPN, Bruyeres le Chatel, 91297 Arpajon, France
3. LPSC, Grenoble, France
4. INRNE, BAS, Sofia, Bulgaria
5. Institute for Nuclear Physics, Cologne, Germany
6. H. Hulubei, NIPNE, Bucharest, Romania
7. Dipartimento di Fisica, Universita di Camerino, Italy
8. Weizmann Institute of Science, Rehovot, Israel
9. University of York, York, United Kingdom
10. Institute Max von Laue-Paul Langevin, Grenoble, France
11. Physik-Department E12, TU Muenchen, Garching, Germany
12. Department of Nuclear Physics, ANU, Canberra, Australia
13. ISOLDE, CERN, Geneva, Switzerland

Spokespersons: G. Georgiev  
Co-Spokespersons: J.M. Daugas, G. Simpson  
Contact person: J. Van de Walle

### Abstract

We propose to study the properties of odd-mass neutron-rich rubidium isotopes by the Coulomb-excitation technique, using the Miniball array coupled to the REX-ISOLDE facility. The results from similar measurements from the recent years (e.g. for the odd-mass and the odd-odd Cu isotopes, IS435) have shown the strong potential in such measurements for gaining information both for single-particle-like and collective states in exotic nuclei. Since there is practically no experimental information for excited states in the odd-mass Rb isotopes beyond <sup>93</sup>Rb, the present study should be able to provide new data in a region of spherical (<sup>93</sup>Rb and <sup>95</sup>Rb) as well as well deformed nuclei (<sup>97</sup>Rb and <sup>99</sup>Rb). Of particular interest is the rapid shape change that occurs when going from <sup>95</sup>Rb ( $\epsilon_2=0.06$ ) to <sup>97</sup>Rb ( $\epsilon_2=0.3$ ). These results should be of significant astrophysical interest as well, due to the close proximity of the r-process path.



## Physics Motivation

The neutron-rich  $A \sim 100$  region of the nuclear chart represents a very interesting ground for testing different theoretical models which should be able to predict both spherical and well deformed nuclear shapes. The nuclei in the neutron-rich  $A \sim 100$  region with 58, or fewer neutrons have spherical ground states. When the number of neutrons increases to 60 the ground state shape suddenly becomes deformed, and nuclei remained deformed, with similar deformations, at higher neutron numbers. This phenomenon was initially indicated through mass measurements [1]. Other experimental evidence for the rapid change in the nuclear deformation has been derived from the quadrupole moment measurements of the ground states of nuclei in this region by laser spectroscopy (e.g. in the Rb isotopes [2]) and excited state lifetime measurements performed over a range of spins for the Sr, Zr and Mo isotopes using plunger [3] and fast-timing techniques [4]. Importantly, shape coexistence has been observed in many of the  $N=59$  nuclei ( $^{99}\text{Zr}$ ,  $^{98}\text{Y}$ ,  $^{97}\text{Sr}$ ,  $^{96}\text{Rb}$ ) which lie on the border of the change in the ground state shapes. Nuclei with  $N=59$  have spherical ground states and deformed rotational bands at higher energies (e.g.  $^{99}\text{Zr}$ , see ref. [5]). The clear identification of bandhead spins, their deformations and the Nilsson orbitals on which they are based in  $N=59$  nuclei has given new insights into the mechanisms responsible for this rapid shape change [5,6] as will be explained in more detail below.

In the past a strong proton-neutron residual interaction between the  $\pi g_{9/2}$  and  $\nu g_{7/2}$  spin-orbit partner orbitals was thought to be responsible for the shape change [7]. This rather selective interaction was later discounted [8] due to the necessity of the inclusion of  $\nu h_{11/2}$  orbitals in calculations of deformed Mo isotopes. It seems the importance of the interaction between the  $\pi g_{9/2}$  and  $\nu g_{7/2}$  orbitals was overstated and was an artifact of the small model space used in the original calculation. This was confirmed by later calculations using a  $^{76}\text{Sr}$  core and a full valence space [9]. More experimental data on the deformation of different proton orbitals would be very useful in order to clearly distinguish the deformation-driving mechanism in the region and reject the above mentioned option of strong interaction between the spin-orbit partners. The refractory nature of many of the elements in this region make their experimental study difficult, however, the Rb isotopes present an ideal case for such studies via Coulomb excitation measurements.

The importance of the unique-parity deformation-driving downsloping  $\nu h_{11/2}$  orbitals around  $N=60$ , which create a low-energy deformed minimum with  $\epsilon_2 \sim 0.4$ , has been stated in many articles [8]. As these orbitals are of unnatural parity they interact little with the neighboring neutron orbitals, but suddenly start to become filled around  $N=60$ , leading to deformation. With this picture consecutive filling of these orbits should produce a gradual progression from a spherical shape to a deformed one, which is not what is experimentally observed. Recently Urban and Pinston have phenomenologically explained this rapid change by invoking the important role played by the  $\nu_{9/2}[404]$  extruder orbital which favors a more spherical shape [5,6]. The observation of shape coexistence in  $^{99}\text{Zr}$ ,  $^{101}\text{Zr}$  and  $^{97}\text{Sr}$ , where different rotational bands have different deformation depending on the orbitals present in the core, points towards this mechanism. In the case of  $^{99}\text{Zr}$ , bands based on the  $\nu_{9/2}[404]$  orbital have the maximum deformation of the region  $\epsilon_2 \sim 0.4$  due to the proximity of the downsloping  $\nu_{1/2}[550]$  and  $\nu_{3/2}[541]$  orbitals to the Fermi surface. In such a band the upsloping  $\nu_{9/2}[404]$  orbital plays only a spectator role. Bands based on either the  $\nu_{1/2}[550]$  or  $\nu_{3/2}[541]$  orbitals were identified to have an intermediate deformation ( $\epsilon_2 \sim 0.3$ ) due to the action of the  $\nu_{9/2}[404]$  orbitals, now present in the core, which work against the deformation. This situation is analogous to the role played by the  $\nu_{11/2}[505]$  orbital in the mass 150 region where nuclei similarly undergo a shape change, as described by Kleinheinz [10]. The works of ref. [5,6] clearly state the

importance of the particular neutron orbitals in this rapid shape change, however it is well known that the proton-neutron interaction plays a major role in the onset of deformation and it would be interesting to see how deformation evolves as  $\pi g_{9/2}$  orbitals are removed. These  $\pi g_{9/2}$  orbitals should interact strongly with the deformation-driving  $\nu h_{11/2}$  orbitals.

Mean field calculations using the Hartree-Fock-Bogoliubov approach based on the D1S Gogny effective nucleon-nucleon interaction and axial symmetric hypothesis[11] show that the changes in the potential energy surface are rather gradual and do not reproduce the experimentally observed sudden change between the spherical and well deformed shapes (see Fig. 1). However, they show well the existence of minima both of prolate and oblate types, consistent with the shape coexistence as discussed in ref. [12] and above.

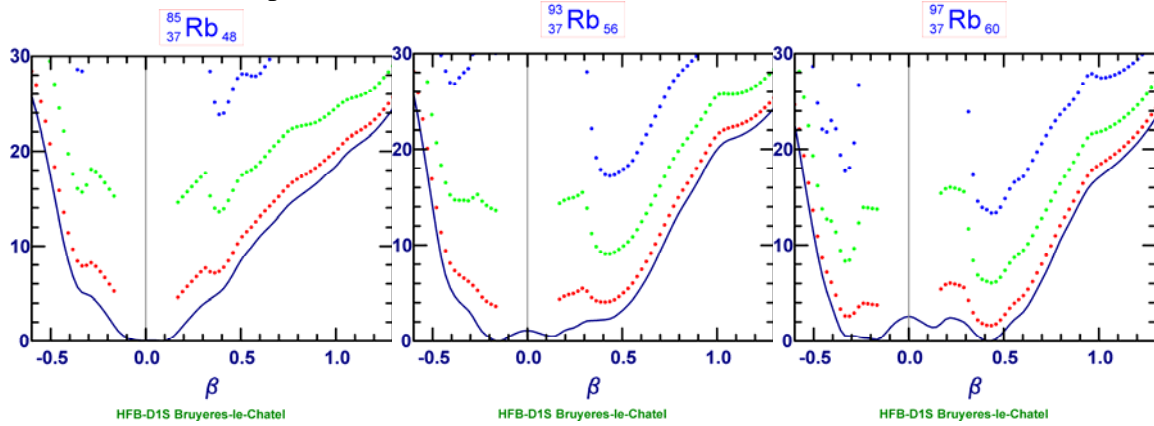


Fig. 1. Potential energy surfaces for the Rb isotopes as derived from ref. [11]

In addition to the HFB calculations, finite-range drop model calculations (FRDM) with a folded-Yukawa single particle potential by Moller, Nix, Myers and Swiatecki [13] predict also a change from a spherical shape to a deformed one as the number of neutrons is increased from 54 to 64. Again this change is gradual rather than rapid. These FRDM calculations are important for astrophysics as they allow  $Q_\beta$  values, ground-state masses, deformations and halflives to be calculated. Although the deformations calculated, using the FRDM, are in good agreement with the measured values for  $^{97}\text{Rb}$  [2], the deviation from the experimental values for  $^{93,95}\text{Rb}$  is rather large and additional experimental information would certainly be useful to confirm this. It is important to test these FRDM calculations whenever possible as any deficiencies in the model could strongly affect predictions for the  $r$ -process paths.

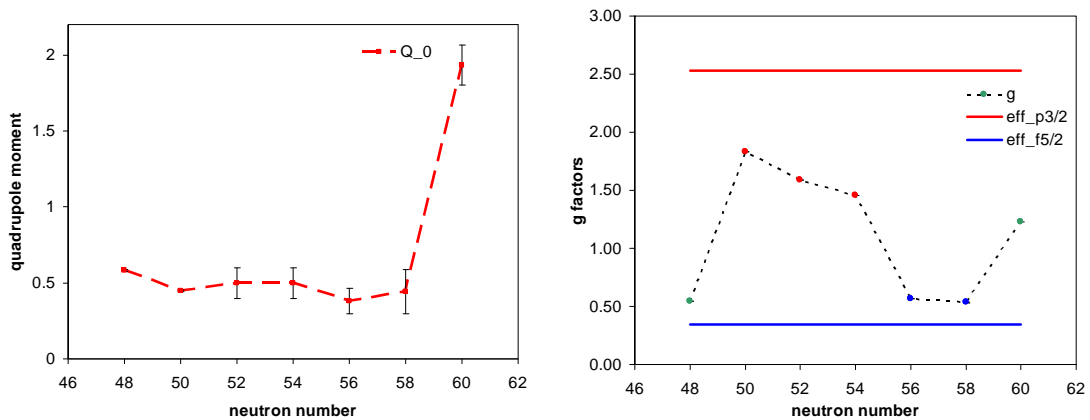


Fig. 2. Experimental ground state quadrupole moments and g factors of the odd-mass Rb isotopes from Ref. [2]. The straight red and blue lines show the effective g factors for the  $\pi p_{3/2}$  and the  $\pi f_{5/2}$  orbitals respectively.

There is significant amount of experimental data for the even-Z nuclei in the region (Kr, Sr), however, the experimental results for the odd-Z Rb isotopes is quite scarce. To the best of our knowledge the last odd-mass Rb isotope with known excited states is  $^{93}\text{Rb}$  [14]. Furthermore the ground-state magnetic and quadrupole moments as well as the hyperfine structures of  $^{93-97}\text{Rb}$  have been measured [2] (see Fig. 2), firmly determining the spin and parity assignments of those states. The magnetic moments of the ground states up to  $A = 95$  ( $N = 58$ ) show behavior not distinctively different from what could be expected for spherical states. The change appears at  $N=60$  with a considerable increase of the quadrupole moment of the ground state. Its g factor can be explained either by the  $\pi_{3/2+}$ [431] or by the  $\pi_{3/2-}$ [301] Nilsson orbitals. From the hyperfine structure studies the spin of the  $^{97}\text{Rb}$  ground state can be unambiguously determined as  $3/2$ , however, its parity cannot be determined. This leaves open the question what is the ordering of the proton orbitals in the well deformed  $^{97}\text{Rb}$ . In order to help resolve this situation we have performed quasi-particle-rotor model calculations to determine the properties of the states involved similar to, but more advanced than, those in [2].

The quasi-particle-rotor model [15] allows the energies, transition probabilities, quadrupole moments and magnetic moments of levels in odd-mass deformed nuclei to be calculated. The input parameters to this model are the strengths of the  $\underline{L}\cdot\underline{g}$  and  $l^2$  terms, which can be obtained by fitting the experimental level spectra of nearby spherical nuclei; the  $\varepsilon_2$ ,  $\varepsilon_4$ ,  $\varepsilon_6$  and  $\gamma$  deformations, an inertia parameter  $a$  (which can be determined from the first  $2^+$  state of the neighboring even-even nucleus) and pairing energy (which can be fixed by looking at the mass differences between neighboring nuclei). We have used this model to calculate the excited states of  $^{97,99}\text{Rb}$ .

As mentioned previously the ground state spin of  $^{97}\text{Rb}$  has been measured to be  $3/2$ , its spectroscopic quadrupole moment  $Q_s=0.586$  eb and its magnetic moment  $\mu=1.894 \mu_N$ . From the quadrupole moment a deformation of  $\varepsilon_2=0.28$  is obtained and used as an input into the calculations. This is close to  $\varepsilon_2=0.317$  predicted by the FRDM calculations [13]. The inertia parameter was fixed using the energy of first  $2^+$  state in  $^{98}\text{Sr}$ . The calculations predict several possible low lying states with spin  $3/2$  with the following properties (see Fig.3).

$I=3/2^-, K=3/2^-$  at 0.0 keV,  $Q_s=0.56$ ,  $\mu=0.60 \mu_N$  (wavefunction 85 %  $3/2$ [301])  
 $I=3/2^+, K=3/2^+$  at 72.1 keV,  $Q_s=0.56$ ,  $\mu=1.92 \mu_N$  (wavefunction 91 %  $3/2$ [431])  
 $I=3/2^-, K=1/2^-$  at 106.5 keV,  $Q_s=-0.54$ ,  $\mu=1.94 \mu_N$  (wavefunction 57 %  $3/2$ [321])

From these predictions the  $\pi_{3/2-}$ [301] state can be ruled out due to the inconsistency between the predicted and observed magnetic moments. The  $\pi_{3/2+}$ [431] and  $\pi_{3/2-}$ [321] have the very similar magnetic moments and the magnitude of their quadrupole moment is almost the same (unfortunately the sign of the quadrupole moment could not be determined in [2]). We have calculated the  $B(E2\uparrow)$  values for  $7/2 \rightarrow 3/2$  transitions for intraband transitions in the bands of interest. The  $B(E2\uparrow)$  values are **0.48  $e^2b^2$**  for the  $7/2 \rightarrow 3/2$  transition in the  $\pi_{3/2+}$ [431] band (108 keV) and **1.02  $e^2b^2$**  for the transition in the  $\pi_{3/2-}$ [321] band (258 keV). A Coulomb-excitation measurement can clearly distinguish between these two possibilities. The transition energies obtained in such a measurement will also allow us to further fine tune the parameters of the model.

The calculations for  $^{99}\text{Rb}$ , performed using the deformations predicted by the FRDM, give the same low-lying Nilsson states as those in  $^{97}\text{Rb}$ ,  $3/2$ [431]  $3/2$ [431],  $1/2$ [321]. Again a  $3/2$  state is predicted to be the lowest lying one for both the positive and negative-parity states. The spectroscopic quadrupole moment is predicted to be the same for both  $3/2$  states (0.67). Again

differing  $B(E2\uparrow)$  values for  $7/2\rightarrow 3/2$  transitions ( $0.67 e^2b^2$   $3/2[431]$ ,  $0.85 e^2b^2$   $3/2[301]$ ,  $1.47 e^2b^2$   $1/2[321]$ ) should allow us to distinguish between these possibilities.

In the case of the lighter, spherical  $^{93,95}\text{Rb}$  isotopes an interpretation in the framework of the shell model is meaningful. Preliminary shell-model calculations have been performed for  $^{93,95}\text{Rb}$  using a  $^{78}\text{Ni}$  inert core and the gwboxg interaction with the NuShellX code [16]. These are able to correctly reproduce the known level scheme.

In the light of the different scenarios discussed above, regarding the cause of the onset of deformation in the  $A = 100$  region, it is important to gain independent information for the active proton orbitals at low excitation energies. One of the most straightforward ways to do this is via a study of the low-energy structure in the odd-proton Rb isotopes. A possibility of obtaining information on the transition probability between the low-energy states in the odd-mass Rb's is certainly an advantage that a Coulomb-excitation study can bring, compared to a beta-decay investigation. As it has been shown in our previous studies in the neutron-rich Cu region [17] in Coulomb-excitation experiment, due to the specific selection rules, one can populate (non-yrast) states that are not observed in beta-decay, deep-inelastic or in spontaneous fission experiments.

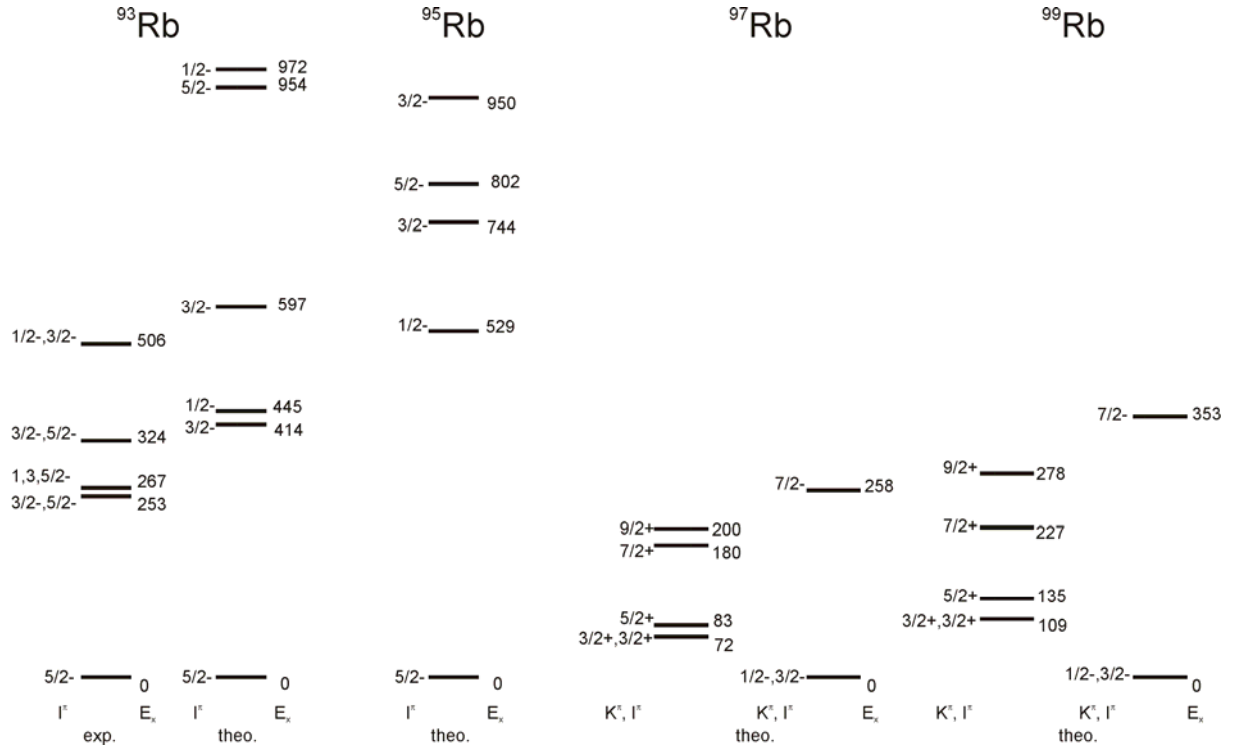


Fig. 3. Level schemes for  $^{93-99}\text{Rb}$ . The theoretical schemes for  $^{93,95}\text{Rb}$  are from shell-model calculations while  $^{97,99}\text{Rb}$  are obtained using the quasi-particle-rotor model.

The aim of the present proposal is to perform a Coulomb excitation study of the  $^{93-99}\text{Rb}$  isotopes. A number of low-energy states are known for  $^{93}\text{Rb}$  (see Fig. 3), although their spin assignments are tentative. This should allow the identification of the highest excitation probability transitions and help the determination of their spins. Following the isotopic chain one should be able, by analogy with  $^{93}\text{Rb}$  and comparison to the shell-model calculations, to identify the low-energy states in the following mostly spherical nucleus  $^{95}\text{Rb}$  before heading to the well deformed  $^{97}\text{Rb}$  and  $^{99}\text{Rb}$ .

It is worth mentioning that the experimentally determined low-energy transitions from this measurement can serve as a starting point for the construction of more detailed level schemes, up to higher spins, using  $\gamma$ - $\gamma$ - $\gamma$  data sets from spontaneous fission and deep-inelastic experiments which lack particle identification.

## Experimental details

The Rb isotopes, post-accelerated by REX-ISOLDE to  $\sim 3$  MeV/A, will be sent to the secondary target, positioned at the Miniball. The gamma-rays from the Coulomb excitation will be detected by the segmented Ge detectors in coincidence with the scattered particles, detected by the double-sided Si strip detector (CD).

The energy of the gamma-rays that we might observe with the Miniball for the chain the Rb isotopes are expected to be in the range  $<100$  keV – 2 MeV with 3 or more gamma transitions expected per isotope. As it has been shown in the Coulomb excitation of the Cu isotopes [17] it might appear necessary to change secondary target (e.g.  $^{104}\text{Pd}$  or  $^{120}\text{Sn}$ ) in order to avoid the overlapping between energies of the target and beam excitation.

During the experiment on the Coulomb excitation of the odd-mass Cu isotopes we have excited levels with energies up to 2 MeV with transition probabilities as low as 3 W.u. Under these conditions we have observed gamma-rays with total intensities, detected in the Miniball array, between few hundreds and few thousands counts in the photopeak. The beam intensities used were about  $1 \times 10^5$  pps –  $2 \times 10^5$  pps. It appeared that these are the maximum beam intensity that can be usually accepted at the Miniball array with target thicknesses of  $\sim 2$  mg/cm<sup>2</sup> without having too high count rate in the CD detector. The typical measurement time for the Cu isotopes was between 24 and 40 hours. Based on this experience we have estimated the necessary beam time for each of the Rb isotopes as presented further.

The neutron-rich rubidium beams are produced at ISOLDE usually using UCx target. Being of alkaline nature, rubidium is one of the elements that are the easiest to extract from the target and is usually considered as one of the main sources of contaminations for other beams. Up to now the Rb beams has been produced using positive surface-ionization ion sources. The data for the available yields, coming from measurements from SC [10] as well as from an old measurement at PSB (target number UC183), is presented in Table 1. Since the carbonization procedure used for the production of UC183 and the one from present days is different we have applied a factor of 10 reduction of the experimental PSB yields [18], already taken into account for the numbers in the table.

*Table 1. ISOLDE yields and count rate estimates for the Rb isotopes at Miniball.*

	ISOLDE yields [p/ $\mu\text{C}$ ]		Expected count rate at Miniball [pps]
	SC	PSB	
$^{93}\text{Rb}$ (5.8 s)	$1 \times 10^8$	$1 \times 10^9$	$> 5 \times 10^6$
$^{95}\text{Rb}$ (377 ms)	$4 \times 10^7$	$1 \times 10^8$	$> 1 \times 10^6$
$^{97}\text{Rb}$ (170 ms)	$5 \times 10^6$	$1 \times 10^7$	$1 \times 10^5$
$^{99}\text{Rb}$ (50 ms)	$4 \times 10^5$	$1 \times 10^5$	$2 \times 10^3$

This shows that the SC numbers should be reproduced nowadays as a minimum approximation. The most probable source of contamination in the Rb beams is the neighboring Sr isotopes. A recent measurement with target UC355 shows that in the worst-case scenario the Sr contamination should be of the order of 5% (data for mass 96) [19]. One

can try to still improve further this ratio by using Ta or Nb transfer lines instead of the W one, used in this measurement.

Due to the use of a surface-ionization ion source in this experiment one would not be able to apply the well established technique of laser-On/laser-Off measurements. However, if a possible Sr contamination appears to be an issue, another approach might be the use of the release-curve technique, applied for  $^{68}\text{Ni}$  as demonstrated in ref. [20]. Due to the considerable difference in the release time of Rb and Sr this should allow an unambiguous identification of the gamma-lines observed in the Coulex spectra as belonging to Rb or to the possible Sr contaminant.

In order to estimate the realistic beam intensities at the Miniball setup we have assumed a standard overall REX-trap + EBIS + LINAC efficiency of 5% for the longer lived states. For the shorter-lived ones one should also take into account the time spent by the nuclei in the REX-trap and the EBIS breeding time that would be in the range of 100 ms – 200 ms and therefore decreasing the estimated overall efficiency to ~2-3% for  $^{97}\text{Rb}$  and 0.5% for  $^{99}\text{Rb}$ . As mentioned above the acceptable beam intensities at the Miniball setup are limited to  $\sim 2 \times 10^5$  pps. These are the maximum values taken into consideration for case of  $^{93}\text{Rb}$  and  $^{95}\text{Rb}$ . We estimate that for performing of the Coulomb-excitation measurement of the odd-mass Rb's we will need:

- 3 shifts of beam on target for  $^{93}\text{Rb}$
- 3 shifts of beam on target for  $^{95}\text{Rb}$
- 3 shifts of beam on target for  $^{97}\text{Rb}$
- 9 shifts of beam on target for  $^{99}\text{Rb}$

Additionally 3 shifts will be necessary for changing between the different isotopes. These sums up to a **total of 21 shifts** request for the Coulomb-excitation measurement of  $^{93-99}\text{Rb}$  isotopes.

## References

- [1] M. Epherre *et al.*, Phys. Rev. **C19**, 1504 (1979)
- [2] C. Thibault *et al.*, Phys. Rev. **C23**, 2720 (1981)
- [3] A.G. Smith *et al.*, J. Phys. **G28**, 2307 (2002)
- [4] H. Mach *et al.*, Phys. Lett. **B230** (1989) 21-26
- [5] W. Urban, J.A. Pinston, Eur. Phys. J. **A16**, 11 (2003)
- [6] W. Urban, Eur. Phys. J. **A22**, 241 (2004)
- [7] P. Federman, S. Pittel, Phys. Lett. **B69**, 385 (1977)
- [8] B. Pfeiffer and K.-L. Kratz in “Nuclear Structure of the Zirconium Region”, Res. Rep. in Phys., Springer-Verlag eds. J. Eberth, R.A. Meyer and K. Sistemich 1988 p. 368
- [9] A. Kumar and M.R. Gunye, Phys. Rev. **C32** (1985) 2116
- [10] P. Kleinheinz *et al.*, Phys. Rev. Lett. **32**, 68 (1974)
- [11] S. Hilaire and M. Girod, Eur. Phys. J. **A33**, 237 (2007); [http://www-phynu.cea.fr/science\\_en\\_ligne/carte\\_potentiels\\_microscopiques/carte\\_potentiel\\_nucleaire\\_eng.htm](http://www-phynu.cea.fr/science_en_ligne/carte_potentiels_microscopiques/carte_potentiel_nucleaire_eng.htm)
- [12] J.L. Wood *et al.*, Phys. Rep. **215**, 101 (1992)
- [13] Moller, Nix, Myers and Swiatecki, At. Data and Nuc. Data Tables **59** (1995) 185
- [14] K.Sistemich *et al.*, Z.Phys. **A325**, 139 (1986)
- [15] P. Semmes and I. Ragnarsson, *The Particle plus Triaxial Model: A Users Guide*, Nuclear Physics Workshop, Oak Ridge 5-16 August 1991 (unpublished)
- [16] NuShellX available at <http://knollhouse.org/default.aspx>
- [17] I. Stefanescu *et al.*, Phys. Rev. Lett. **100**, 112502 (2008)
- [18] H.-J. Kluge (editor) ISOLDE Guide for Users; CERN 86-05 (1986)
- [19] T. Stora, *private communication*
- [20] N. Bree *et al.*, Phys. Rev. **C 78**, 047301 (2008)